



# Investigation on the radiocesium transfer to rice plants near the water inlet of paddy fields via an in situ experiment using non-contaminated soil

Anastasiia Klevtsova<sup>1</sup> · Rinji Inaba<sup>1</sup> · Moeka Takahashi<sup>1</sup> · Yoshimasa Suzuki<sup>1</sup> · Susumu Miyazu<sup>2</sup> · Kazuki Suzuki<sup>3</sup> · Naoki Harada<sup>2</sup> · Norio Nogawa<sup>4</sup> · Tatsuhiro Nishikiori<sup>5</sup> · Tomijiro Kubota<sup>6</sup> · Natsuki Yoshikawa<sup>2</sup>

Received: 30 May 2022 / Accepted: 13 July 2022 / Published online: 11 August 2022  
© Akadémiai Kiadó, Budapest, Hungary 2022

## Abstract

An in situ model paddy field experiment was conducted using non-contaminated soil to identify factors that locally increase the radiocesium activity concentrations in rice near the water inlet of paddy fields. The results demonstrated that irrigation water intake reduced exchangeable potassium concentration and increased radiocesium activity concentration in the soil near the water inlet; thus, the radiocesium activity concentration in rice was negatively correlated with the former and positively with the latter. Exchangeable potassium flushing and deposition of suspended solids in the soil owing to irrigation water intake facilitated the transfer of radiocesium to rice plants near the water inlet.

**Keywords** Radiocesium · Fukushima Dai-ichi Nuclear Power Plant accident · Irrigation water · Model paddy field · Contaminated soil · Rice plant

## Introduction

After the TEPCO Fukushima Dai-ichi Nuclear Power Plant (FDNPP) accident in 2011, caused by a massive earthquake and the associated tsunami, radioactive materials were released into the atmosphere and descended over a wide area

of eastern Japan, mainly in Fukushima Prefecture. Among the released radionuclides, radioactive cesium-137 (<sup>137</sup>Cs) has a half-life of 30.2 years; hence, a long-term impact over a wide area is expected [1, 2].

Contamination by radioactive substances includes direct pollution via radioactive fallout and indirect pollution via the transportation of the radioactive fallout through water basins. Moreover, because large amounts of water are used for irrigation in paddy fields, there is direct contamination due to direct adhesion of radioactive fallout to crops, indirect contamination due to absorption of radiocesium by the soil, and indirect contamination through irrigation systems [3–6]. Various authors have reported that the presence of <sup>137</sup>Cs in irrigation water can significantly increase <sup>137</sup>Cs accumulation in rice plants [7–10]. Following the FDNPP accident, Endo et al. [11] found higher radiocesium contamination in rice from paddy fields irrigated with dam water than in those from the fields irrigated with groundwater.

In general, <sup>137</sup>Cs in water is broadly classified into dissolved and particulate forms [12–14]. The dissolved form exists in an ionic state in water and is known to be highly bioavailable [15, 16], while the particulate form is bound to suspended solids in water [17]. Particulate <sup>137</sup>Cs is strongly fixed to soil particles, and its bioavailability is extremely low. However, the ion-exchanged or organic-bonded forms

✉ Natsuki Yoshikawa  
natsuky@agr.niigata-u.ac.jp

<sup>1</sup> Graduate School of Science and Technology, Niigata University, 8050 Ikarashi 2-no-cho, Nishi-ku, Niigata 950-2181, Japan

<sup>2</sup> Institute of Science and Technology, Niigata University, 8050 Ikarashi 2 no-cho, Nishi-ku, Niigata 950-2181, Japan

<sup>3</sup> Institute for Research Promotion, Niigata University, 8050 Ikarashi 2 no-cho, Nishi-ku, Niigata 950-2181, Japan

<sup>4</sup> Isotope Science Center, The University of Tokyo, 2-11-16 Yayoi, Bunkyo-ku, Tokyo 113-0032, Japan

<sup>5</sup> Agricultural Radiation Research Center, Tohoku Agricultural Research Center, National Agriculture and Food Research Organization, 50 Harajukuminami, Arai, Fukushima-shi, Fukushima 960-2156, Japan

<sup>6</sup> Institute for Rural Engineering, National Agriculture and Food Research Organization, 2-1-6 Kannondai, Tsukuba, Ibaraki 305-8609, Japan

can switch to an ionic state through ion exchange and organic matter decomposition of the bound soil particles [18].

Some studies have reported that the amount of  $^{137}\text{Cs}$  introduced via irrigation water is negligibly less than that originally present in non-contaminated paddy fields [19, 20]. Contrastingly, Sakai et al. [21] reported that the activity concentrations of  $^{137}\text{Cs}$  in topsoil increased by 3.8 times in decontaminated paddy fields 1 year after the removal of topsoil via irrigation water withdrawal and atmospheric deposition. Although the removal measures were effective in reducing  $^{137}\text{Cs}$  uptake, the  $^{137}\text{Cs}$  activity concentration in rice plants increased. This may be related to the  $^{137}\text{Cs}$  present in irrigation water [22].

According to Yoshikawa et al. [23], in paddy fields, the water inlet area is the most contaminated with  $^{137}\text{Cs}$ , where elevated  $^{137}\text{Cs}$  activity concentrations have been detected in both paddy soil and brown rice. This suggests that both dissolved and particulate forms of  $^{137}\text{Cs}$  may contribute to the increase in  $^{137}\text{Cs}$  activity concentration in rice; however, the contributing factors and mechanisms are still largely unknown. The main purpose of this study was to elucidate the factors that increase the activity concentration of  $^{137}\text{Cs}$  in rice due to irrigation water using an in situ model paddy field experiment.

## Experimental

### Study site

The study area ( $37^{\circ} 29' 59'' \text{ N}$ ,  $140^{\circ} 58' 26'' \text{ E}$ ) is located in Namie Town, Fukushima Prefecture, approximately 10 km northwest of FDNPP ( $37^{\circ} 25' 17'' \text{ N}$ ,  $141^{\circ} 01' 58'' \text{ E}$ ) (Fig. 1). This area was designated as a restricted cropping zone during August 2013–March 2017. Rice cultivation in the study paddy field was suspended for 3 years immediately after the FDNPP accident, and trial cultivation was restarted in 2015. These paddy fields were irrigated with water from the Ukedo River supplied by the Ogaki Dam. The catchment area of the Ogaki Dam includes a highly contaminated area where  $^{137}\text{Cs}$  accumulated at  $100\text{--}3000 \text{ kBq m}^{-2}$  due to the influence of radioactive plume passing immediately after the FDNPP accident [24, 25], and the air dose rate was  $0.2\text{--}19.0 \mu\text{Sv h}^{-1}$  (as of November 4, 2015; Nuclear Regulation Authority). The soil type was categorized as coarse-grained brown lowland soil (Institute for Agro-Environmental Sciences, NARO, 2010). In 2015, the radiocesium concentration found in brown rice did not exceed  $100 \text{ Bq kg}^{-1}$ .

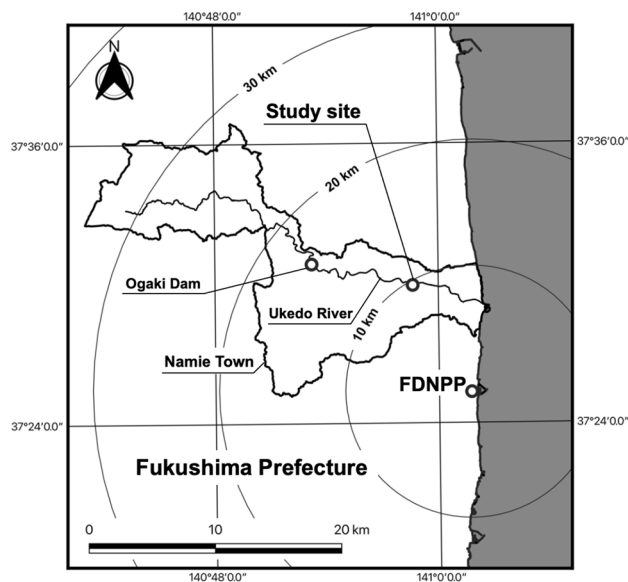


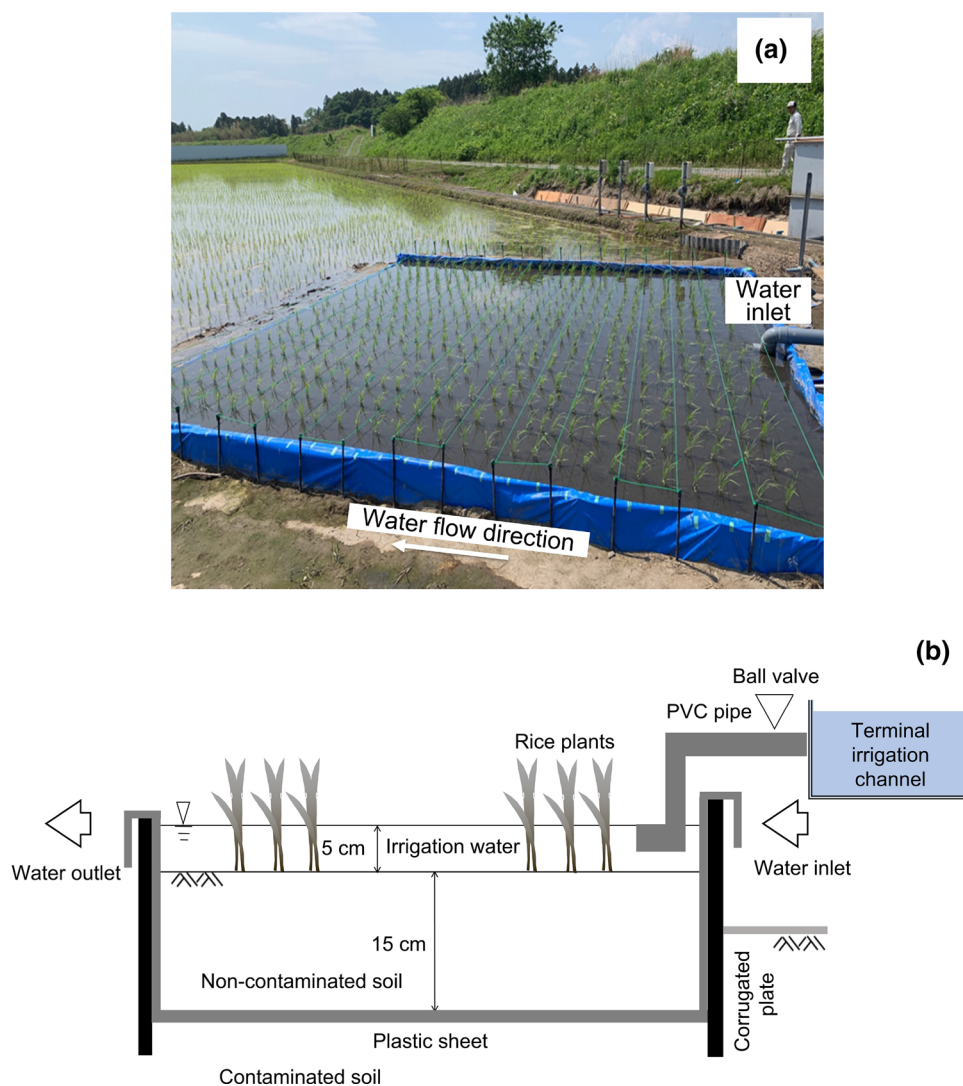
Fig. 1 Map of the study area

### Study method

To elucidate the mechanism by which rice plants absorb the  $^{137}\text{Cs}$  introduced from irrigation water, a field experiment was conducted to observe the sedimentation of suspended solids onto the paddy soil and the changes in exchangeable potassium (hereafter Ex-K) concentrations in the soil.

A  $5 \text{ m} \times 5 \text{ m}$  experimental model paddy field was set up using corrugated plates at the water inlet in 2019 (Fig. 2a). As soil contamination with  $^{137}\text{Cs}$  by irrigation water was locally significant up to 3 m from the water inlet [23], we considered this dimension to be sufficient for measuring the extent of soil contamination near the water inlet. The experimental model paddy field site was dug to a depth of approximately 5 cm and surrounded on all sides by 25 cm high polypropylene corrugated plates. The side plates of the experimental site were set at a height that would allow a water depth of approximately 10 cm to be stored so that water would not overflow. The downstream plates perpendicular to the flow direction were set approximately 5 cm lower than the sides plates to allow irrigation water to flow down without stagnation. A plastic sheet was placed at the bottom to prevent mixing with local soil, and the site was filled to the top 15 cm with approximately 7 tons of non-contaminated paddy soil ( $497 \text{ Bq m}^{-2}$  or less) collected from Shibata City, Niigata Prefecture (Fig. 2b). The physical and chemical properties of the soil are shown in the supplementary material (Appx. 1). We used non-contaminated soil as a fill material because the inventory of  $^{137}\text{Cs}$  in the local paddy soil ( $\sim 59,800 \text{ Bq m}^{-2}$  as in

**Fig. 2** **a** Photograph of the experimental model paddy field; **b** schematic of the experimental model paddy field



2018) was considerably greater than the particulate  $^{137}\text{Cs}$  inflow via irrigation water ( $\sim 300 \text{ Bq m}^{-2}$  as in 2018), and it was expected that it might be difficult to identify the changes in soil  $^{137}\text{Cs}$  activity concentration due to irrigation water intake.

Nitrogen (N), phosphorus (P), and potassium (K) fertilizers were applied according to the Fukushima Prefecture fertilization standard for paddy fields ( $6 \text{ g m}^{-2}$  for N,  $8 \text{ g m}^{-2}$  for P, and  $10 \text{ g m}^{-2}$  for K) [26]. Irrigation water was supplied through a PVC pipe ( $\phi 100 \text{ mm}$ ) connected to the existing water inlet. The flow rate was adjusted using a ball valve attached to the PVC pipe, and a flow meter (SW100G-M, Aichi Tokei Denki Co., Ltd.) was installed to measure and record the flow rate every 10 min throughout the irrigation period. The experimental model paddy field was irrigated with water from the Kariyado Headwork, located approximately 7 km downstream from the Ogaki Dam. The water was transported to the fields

through an open irrigation channel in 2019, for the first time since the 2011 Great East Japan earthquake.

Puddling was performed manually using hoes and scoop shovels. After the disturbing muddy water had settled, the rice seedlings (*Oryza sativa* L., Koshihikari) were transplanted, with a spacing of 15 cm, in the direction of irrigation flow and 30 cm in the cross direction, similar to that in the local field.

### Sampling

The soil and rice were sampled on September 24, 2019. Sampling sites were set up by dividing the experimental model paddy field into several grids of three different sizes. We wanted to sample densely near the water inlet, where the sedimentation of particulate radiocesium is expected to be greater, based on the results of the model paddy field experiment conducted under laboratory conditions in 2018 (Appx.

2). Therefore, we set up  $0.25\text{ m} \times 0.25\text{ m}$  grids covering  $1\text{ m}$  width and  $2\text{ m}$  downstream from the water inlet (hereinafter Zone 1),  $0.5\text{ m} \times 0.5\text{ m}$  grids surrounding Zone 1 (hereinafter Zone 2), and  $1\text{ m} \times 1\text{ m}$  grids furthest from the water inlet (hereinafter Zone 3) (Fig. 3a). Three soil samples ( $5\text{ cm}$  depth each) were collected from the center of each sampling grid using a core sampler ( $5\text{ cm}$  diameter,  $5.1\text{ cm}$  long; DIK-1801, Daiki Rika Kogyo Co Ltd., Saitama, Japan).

For rice plant sampling, as there was only one rice plant hill in the smallest grid (Zone 1), two  $0.25\text{ m} \times 0.25\text{ m}$  grids

were combined. Thus, two rice plant hills were sampled from the smallest grids. For the middle- and large-sized grids (Zone 2 and 3, respectively), four rice plant hills from the center of each grid were selected for sampling (Fig. 3b).

Water samples were collected from the terminal irrigation channel near the experimental model paddy field once a month during the irrigation season between May and September 2019. Each time,  $60\text{ L}$  of water samples was collected. Samplings were performed on days when it had not rained for at least 2 days prior.

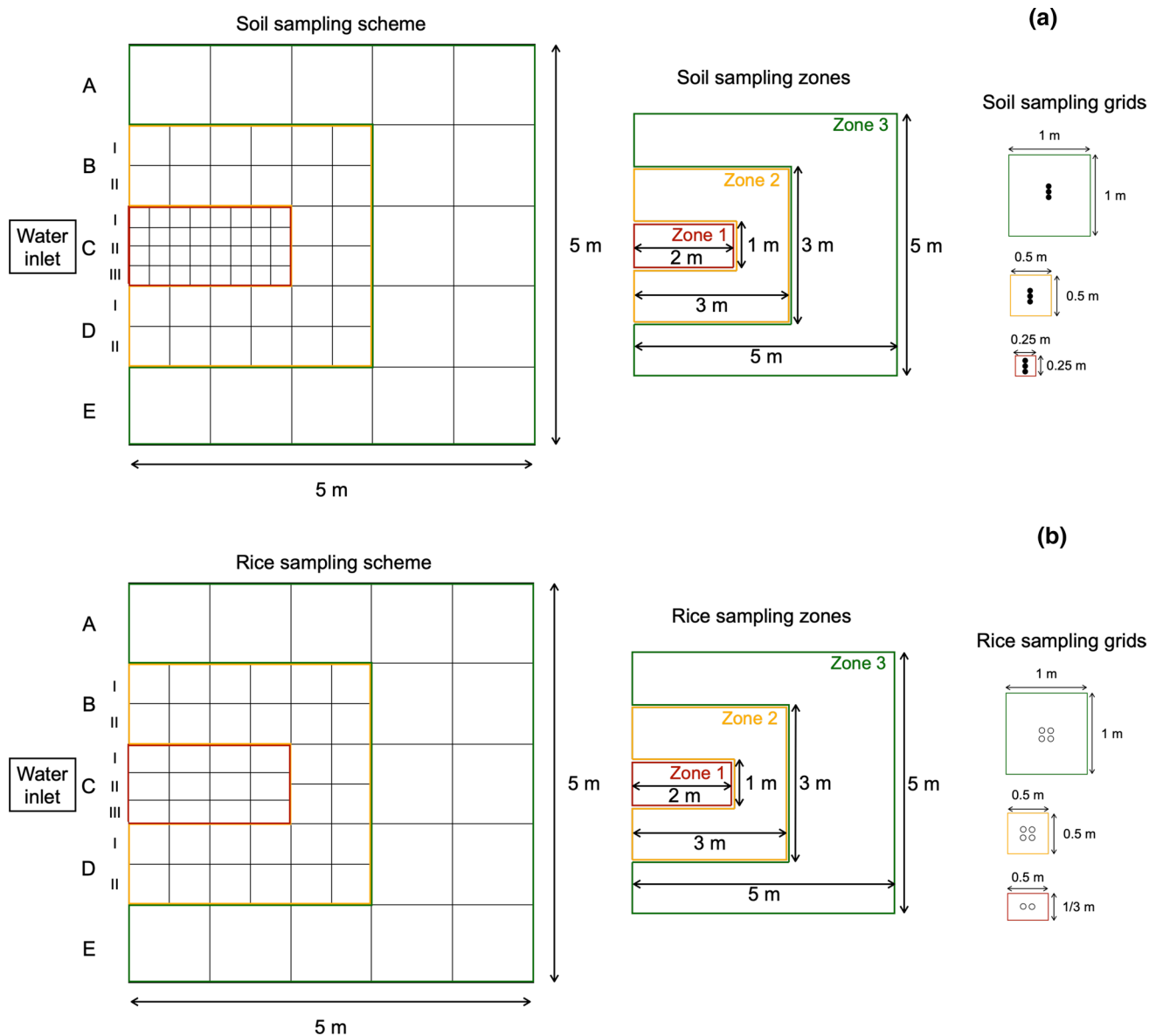


**Fig. 3** Soil and rice sampling sites. The size of the experimental model paddy field was  $5\text{ m} \times 5\text{ m}$ . The sampling sites were set up by dividing the total field into three different sized grids: **a** for soil sampling:  $0.25\text{ m} \times 0.25\text{ m}$  grids covering  $2\text{ m}$  downstream and  $1\text{ m}$  wide from the water inlet (Zone 1),  $0.5\text{ m} \times 0.5\text{ m}$  grids surrounding Zone 1 (Zone 2), and  $1\text{ m} \times 1\text{ m}$  grids furthest from the water inlet (Zone

3)—three samples were collected from each grid; **b** for rice sampling: two  $0.25\text{ m} \times 0.25\text{ m}$  grids (Zone 1) were combined, and two rice plant hills were sampled; in  $0.5\text{ m} \times 0.5\text{ m}$  and  $1\text{ m} \times 1\text{ m}$  grids (Zone 2 and 3, respectively), four rice plant hills from the center of each grid were sampled. “A–E” indicate horizontal grid locations from the water inlet, “I–III” indicate finer grid distribution

## Pre-treatment of samples

According to Kato et al. [27], approximately 80% of the dissolved and particulate  $^{137}\text{Cs}$  was present in the top 2 cm of the topsoil. Given that the particulate  $^{137}\text{Cs}$  introduced via irrigation water was thinly deposited on the soil surface, only the top 2 cm of the collected soil samples was used for analysis. Soil samples were absolutely dried in an electric oven and then homogenized by stirring to ensure uniform  $^{137}\text{Cs}$  activity concentration.

Rice plants were air-dried in a greenhouse for approximately 2 weeks, threshed manually, and separated into straws and grains. Rice grains were threshed until unhulled. Soil and rice grain samples were weighed and transferred to a U-8 container for  $^{137}\text{Cs}$  activity determination.

The dissolved and particulate fractions of irrigation water samples were separated and prepared for dissolved and particulate  $^{137}\text{Cs}$  analyses, as described by Yoshikawa et al. [23].

## $^{137}\text{Cs}$ activity measurement

The  $^{137}\text{Cs}$  activity concentrations of all the soil, rice and water samples were measured at the Isotope Research Center of the University of Tokyo. A germanium semiconductor detector with 25% efficiency and a counting time of 14,400 s (Princeton Gamma-Tech Instruments Inc., MCA8016, Princeton, NJ, USA) was used to determine the radiocesium activity in water and rice samples. An NaI (TI) scintillation detector with a counting time of 3600 s (AT-1320A, ATOM-TEX, Minsk, Belarus or WIZARD-2, PerkinElmer Co., MA, USA) was used to determine the radiocesium activity in the soil. The counting efficiency of the detectors was calibrated using a gamma-ray reference source (MX033U8PP; Japan Radioisotope Association, Tokyo, Japan). The counting periods were chosen to ensure that the limit of quantitation was 0.1 Bq kg<sup>-1</sup> for the water and rice plant samples and 30 Bq kg<sup>-1</sup> for the soil samples. The  $^{137}\text{Cs}$  activity concentrations of all the samples were decay-corrected to April 1, 2019.

## Determination of Ex-K

The Ex-K in paddy field soil was determined by soil extraction with 30 mL of 1 M ammonium acetate ( $\text{CH}_3\text{COONH}_4$ ) at 20 °C while shaking for 1 h. The suspension was centrifuged (3000 rpm) for 15 min, then the supernatant was filtered using cellulose acetate syringe filters (13 mm; ADVANTEC, Osaka, Japan). The filtrate was diluted with 0.1 N  $\text{HNO}_3$  for Ex-K determination using an atomic

absorption spectrophotometer (ZA-3300 Hitachi High-Tech Science Corporation, Tokyo, Japan).

## Statistical analysis

Statistical analysis was performed for radiocesium activity concentration in the soil and rice and for Ex-K in the soil using the R statistical software (version 3.5.2; R Foundation for Statistical Computing, Vienna, Austria). We compared the data sets of Zones 1–3 using the pairwise Wilcoxon rank-sum test with Benjamini–Hochberg correction ( $p < 0.05$ ) for multiple comparisons.

## Results and discussion

The results demonstrated that the unhulled rice grains harvested near the water inlet (Zone 1) had significantly higher  $^{137}\text{Cs}$  activity concentrations than those in the other zones. In this section, the reasons for the high radiocesium contamination in rice locally near the water inlet are discussed from the perspectives of (1) reduced soil Ex-K and (2) increased  $^{137}\text{Cs}$  activity concentrations in the soil due to irrigation water intake.

### Effect of soil runoff on Ex-K

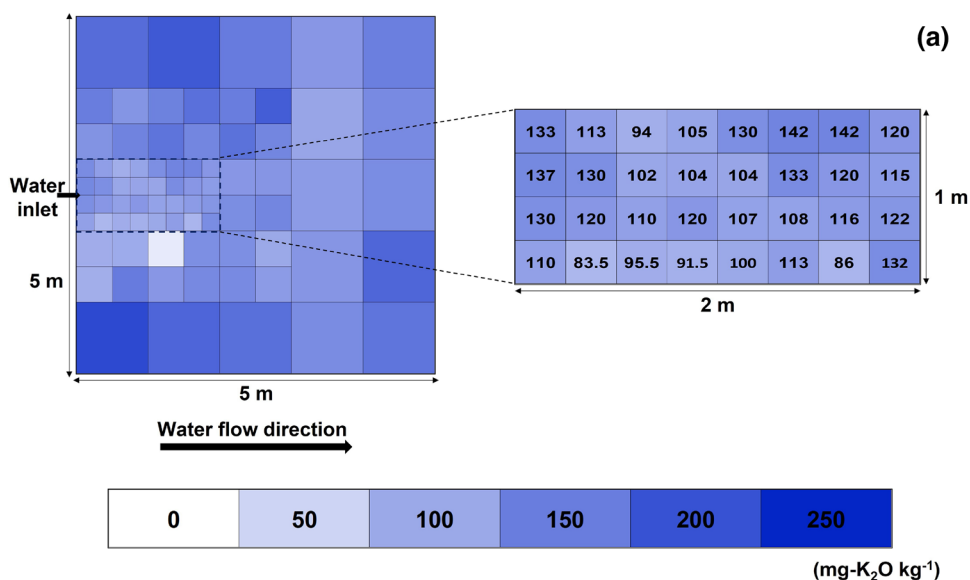
The highest average Ex-K concentration of 151 mg-K<sub>2</sub>O kg<sup>-1</sup> was found in Zone 3 and the lowest of 115 mg-K<sub>2</sub>O kg<sup>-1</sup> in Zone 1 (Fig. 4a). We observed a significantly lower concentration of Ex-K in Zone 1 than in the other zones ( $p < 0.05$ , Wilcoxon's test) (Fig. 4b). The reason for the low Ex-K near the water inlet could be that the continuous turbulent water flow had leached the applied Ex-K downstream. It is well known that there is a negative correlation between Ex-K in the soil and  $^{137}\text{Cs}$  absorption by rice plants [28–32]. Therefore, it is plausible that relatively low Ex-K concentrations contributed to the elevated  $^{137}\text{Cs}$  activity concentrations in rice grains.

### Effects of newly added $^{137}\text{Cs}$ via irrigation water

#### Possibility of direct absorption of dissolved radiocesium by rice plants

The average activity concentration of  $^{137}\text{Cs}$  in irrigation water was 1.76 Bq L<sup>-1</sup>, of which dissolved form was  $1.57 \pm 0.20$  Bq L<sup>-1</sup> and particulate form was  $0.19 \pm 0.13$  Bq L<sup>-1</sup>. As dissolved  $^{137}\text{Cs}$  has high bioavailability, we would like to discuss the possibility of direct absorption of dissolved  $^{137}\text{Cs}$  in irrigation water by rice plants. Yoshikawa et al. [23] reported that the activity concentration of dissolved  $^{137}\text{Cs}$  tends to decrease at a constant rate

**Fig. 4** Exchangeable K (Ex-K) in the soil collected on September 24, 2019 (harvesting season) (Appx. 3): **a** distribution of Ex-K in the experimental model paddy field indicating low (light colors) to high (dark blue) values; **b** comparison of Ex-K concentration in the three zones;  $n$ =number of grids,  $n=32$  for Zone 1,  $n=28$  for Zone 2,  $n=16$  for Zone 3; lowercase letters indicate the significant differences between each zone at  $p<0.05$  using pairwise Wilcoxon rank-sum test with Benjamini–Hochberg correction for multiple comparisons. Means sharing a letter are not significantly different. (Color figure online)

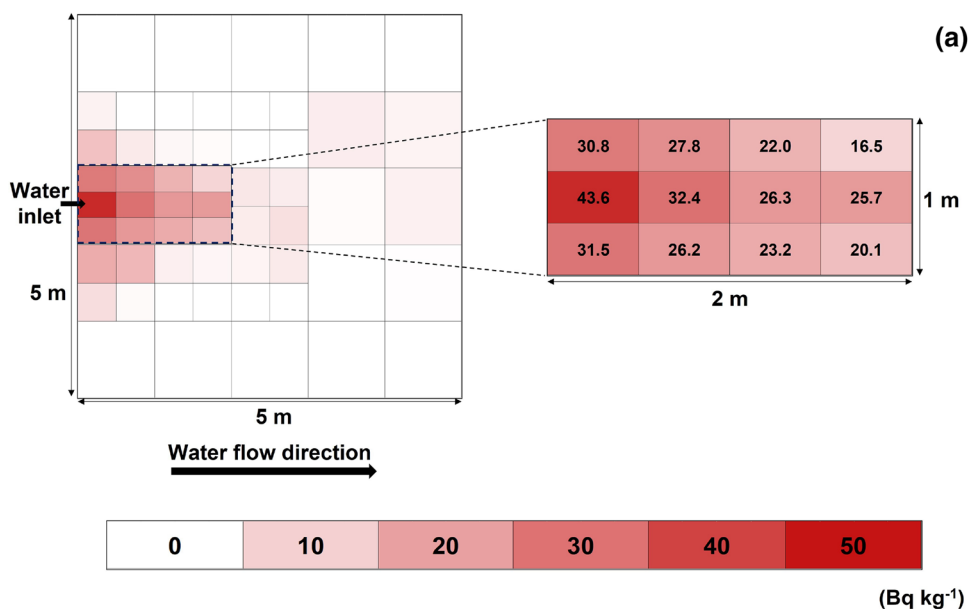


during the flow from the inlet to the outlet. If absorption by rice plants is responsible for this decrease, then rice plants would have a uniform activity concentration regardless of the distance from the inlet. However, in the present experiment, the <sup>137</sup>Cs activity concentration in rice grains in Zone 1 ( $27.2 \pm 7.0$  Bq kg<sup>-1</sup>) was significantly higher than that in Zones 2 ( $11.3 \pm 4.1$  Bq kg<sup>-1</sup>) and 3 ( $9.3 \pm 2.3$  Bq kg<sup>-1</sup>) ( $p < 0.05$ , Wilcoxon's test) (Fig. 5b). Thus, while dissolved <sup>137</sup>Cs in the irrigation water may contribute to the uniform increase in activity concentration throughout the experimental system, the local increase around the inlet cannot be explained by dissolved <sup>137</sup>Cs alone.

The transfer factors (TFs), calculated as the ratio of <sup>137</sup>Cs activity concentration in rice to that in the soil,

were 0.001–0.004 for Zone 1, 0.001–0.087 for Zone 2, and 0.005–1.423 for Zone 3 (Appx. 3). The high TFs in Zone 3 cannot be explained by transfer from the soil alone; direct absorption from irrigation water may also have contributed. In other words, dissolved radiocesium may have a bottom-up effect on the activity concentration in rice throughout the experimental system. Therefore, dissolved radiocesium did not seem to be the main reason for the increase <sup>137</sup>Cs activity concentrations in rice plants near the water inlet (Zone 1) (Fig. 5a), although dissolved <sup>137</sup>Cs could contribute partly to increasing the activity concentration of <sup>137</sup>Cs in rice plants.

**Fig. 5.**  $^{137}\text{Cs}$  activity concentration in the unhulled rice grains from plants cultivated in the experimental model paddy field, collected on September 24, 2019 (harvesting season) (Appx. 3): **a** distribution of  $^{137}\text{Cs}$  in the experimental model paddy field indicating low (light colors) to high (dark red) values; **b** comparison of  $^{137}\text{Cs}$  concentrations among the three zones;  $n$  = number of grids,  $n = 12$  for Zone 1,  $n = 28$  for Zone 2,  $n = 16$  for Zone 3; lowercase letters indicate the significant differences between each zone at  $p < 0.05$  using pairwise Wilcoxon rank-sum test with Benjamini–Hochberg correction for multiple comparisons. Means sharing a letter are not significantly different. (Color figure online)



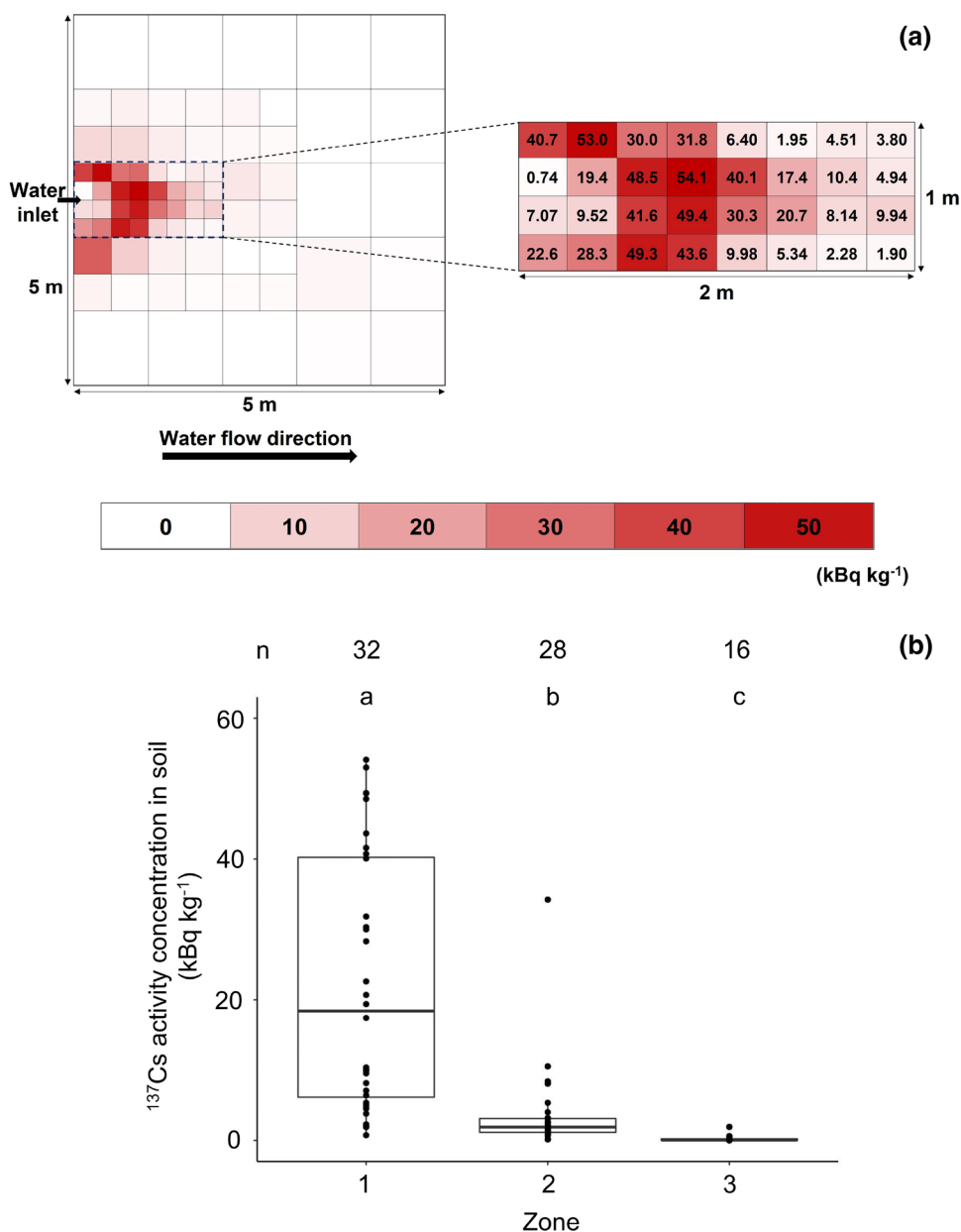
### Soil $^{137}\text{Cs}$ inventory increases via irrigation water

The highest average activity concentration of  $22.1 \text{ kBq kg}^{-1}$  in the soil was found near the water inlet (Zone 1) and the lowest of  $0.25 \text{ kBq kg}^{-1}$  in the outer periphery area (Zone 3) (Fig. 6a). The value for Zone 1 was significantly higher than the values for other zones ( $p < 0.05$ , Wilcoxon's test) (Fig. 6b). These findings suggested that the rice plants near the water inlet were exposed to an environment wherein they were more likely to absorb  $^{137}\text{Cs}$  than those at other locations. A significant positive correlation ( $p < 0.05$ , Pearson's test) was observed between the  $^{137}\text{Cs}$  inventory in the soil and  $^{137}\text{Cs}$  activity concentration in rice grains at each

sampling point during the harvesting period (Fig. 7). Given that the experimental model paddy field was filled with non-contaminated paddy soils, one of the main factors explaining the increase in soil  $^{137}\text{Cs}$  inventory near the water inlet was the deposition of particulate  $^{137}\text{Cs}$  from the irrigation water intake.

The primary hypothesis regarding the significantly higher  $^{137}\text{Cs}$  activity concentrations in the soil is that the suspended solids transported by water in the fast-flowing irrigation channel are deposited near the water inlet owing to a sudden decrease in the tractive force of the irrigation water flow immediately after it enters the paddy field. To verify this hypothesis, the inflow load of particulate  $^{137}\text{Cs}$  via irrigation

**Fig. 6.**  $^{137}\text{Cs}$  activity concentration in each grid of the experimental model paddy field soil collected on September 24, 2019 (harvesting season) (Appx. 3): **a** distribution of  $^{137}\text{Cs}$  in the field indicating low (light colors) to the higher (dark red) values; **b** comparison of  $^{137}\text{Cs}$  concentrations among the three zones;  $n$  = number of grids,  $n = 32$  for Zone 1,  $n = 28$  for Zone 2,  $n = 16$  for Zone 3; lowercase letters indicate significant differences between each zone at  $p < 0.05$  using pairwise Wilcoxon rank-sum test with Benjamini–Hochberg correction for multiple comparisons. Means sharing a letter are not significantly different. (Color figure online)



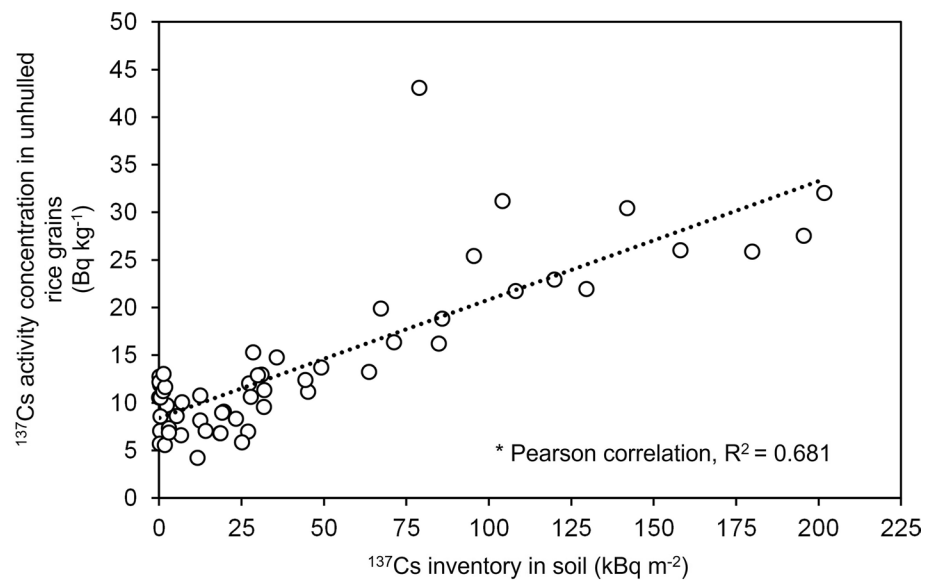
water and the increase in the  $^{137}\text{Cs}$  inventory in the experimental model paddy soil were calculated and compared. The increase in  $^{137}\text{Cs}$  activity concentration in the soil was calculated as the difference between the  $^{137}\text{Cs}$  inventories in the soil during the transplantation and harvesting periods. The inventory of  $^{137}\text{Cs}$  in the soil was calculated by multiplying the activity concentration in each grid, represented by each sampling point, by the mass of the dry soil and then adding them. The total particulate  $^{137}\text{Cs}$  inflow load was calculated by multiplying the amount of water intake by the  $^{137}\text{Cs}$  activity concentration in the suspended solids during the irrigation period.

Consequently, the total increase in  $^{137}\text{Cs}$  inventory in soil was 538 kBq. This value represents  $\sim 60\%$  of the total

particulate  $^{137}\text{Cs}$  inflow load [889 kBq, average activity concentration ( $0.19 \text{ Bq L}^{-1}$ ) multiplied by the intake water volume ( $4.68 \times 10^6 \text{ m}^3$ )]. Therefore, the increase in soil  $^{137}\text{Cs}$  inventory can reasonably be attributed to the sedimentation of suspended solids via irrigation water inflow. Accordingly, it was suggested that particulate radiocesium was one of the main causes of the increase in  $^{137}\text{Cs}$  concentrations in rice plants near the water inlet.



**Fig. 7** Correlation between  $^{137}\text{Cs}$  inventory in the soil and  $^{137}\text{Cs}$  activity concentration in the unhulled rice grains in each grid of the experimental model paddy field



## Conclusions

In this study, we attempted to elucidate the factors that contribute to the elevated radiocesium activity concentration in rice derived from irrigation water intake. In the experimental model paddy field with non-contaminated soil,  $^{137}\text{Cs}$  activity concentration in the soil and harvested rice was significantly higher, and Ex-K in the soil was significantly lower near the water inlet (Zones 1) than at other locations (Zones 2 and 3).

The reason for the low Ex-K near the water inlet may be the continuous turbulent water flow leaching the Ex-K downstream, which could partially explain the contribution of radiocesium to rice absorption. On the other hand, the strong correlation between  $^{137}\text{Cs}$  activity concentration in the soil and  $^{137}\text{Cs}$  activity concentration in the rice clearly indicates that the elevated concentrations in the soil contribute to the increased  $^{137}\text{Cs}$  absorption by rice. It can be considered that the dissolved radiocesium increased the concentration of radiocesium in rice plants bottom-up in the entire experimental system, whereas particulate  $^{137}\text{Cs}$  increased its concentration in the soil locally near the water inlet, which was then absorbed by rice plants.

**Supplementary Information** The online version contains supplementary material available at <https://doi.org/10.1007/s10967-022-08448-1>.

**Acknowledgements** The authors would like to acknowledge and extend their profound gratitude to the farmers in Namie Town for their support and provision of the experimental paddy fields. This research was financially supported by a Grants-in-Aid for Scientific Research (No. JP19H03072) from the Japan Society for the Promotion of Science.

**Author contributions** All authors contributed to the study conception and design. Material preparation, data collection and analysis were performed by AK, RI, MT and YS. The investigation of the model paddy field experiment was performed with the involvement of TN

and TK. The  $^{137}\text{Cs}$  activity concentration of samples was measured under the direction of NN. The data curation was performed by KS, SM and NH. The first draft of the manuscript was written by AK and all authors commented on previous versions of the manuscript. The final manuscript was reviewed and edited by NY. The all authors read and approved the final manuscript.

## Declarations

**Conflict of interest** The authors declare no conflicts of interest associated with this manuscript.

## References

1. Yasunari TJ, Stohl A, Hayano RS et al (2011) Cesium-137 deposition and contamination of Japanese soils due to the Fukushima nuclear accident. *Proc Natl Acad Sci USA* 108:19530–19534. <https://doi.org/10.1073/pnas.1112058108>
2. Saito K, Tanihata I, Fujiwara M et al (2015) Detailed deposition density maps constructed by large-scale soil sampling for gamma-ray emitting radioactive nuclides from the Fukushima Dai-ichi Nuclear Power Plant accident. *J Environ Radioact* 139:308–319. <https://doi.org/10.1016/j.jenvrad.2014.02.014>
3. Harada N, Nonaka M (2012) Soil radiocesium distribution in rice fields disturbed by farming process after the Fukushima Dai-ichi Nuclear Power Plant accident. *Sci Total Environ* 438:242–247. <https://doi.org/10.1016/j.scitotenv.2012.05.032>
4. Yoshikawa N, Obara H, Ogasa M et al (2014)  $^{137}\text{Cs}$  in irrigation water and its effect on paddy fields in Japan after the Fukushima nuclear accident. *Sci Total Environ* 481:252–259. <https://doi.org/10.1016/j.scitotenv.2014.01.129>
5. Fesenko S, Shinano T, Onda Y, Dercon G (2020) Dynamics of radionuclide activity concentrations in weed leaves, crops and of air dose rate after the Fukushima Daiichi Nuclear Power Plant accident. *J Environ Radioact* 222:106347. <https://doi.org/10.1016/j.jenvrad.2020.106347>
6. Konoplev A, Wakiyama Y, Wada T et al (2021) Radiocesium distribution and mid-term dynamics in the ponds of the Fukushima Dai-ichi nuclear power plant exclusion zone in 2015–2019.

- Chemosphere 265:129058. <https://doi.org/10.1016/j.chemosphere.2020.129058>
7. Myttenaere G, Bourdeau P, Masset M (1969) Relative importance of soil and water in the indirect contamination of flooded rice with radiocaesium. *Health Phys* 16:701–707
  8. Nakanishi TM, Kobayashi NI, Tanoi K (2013) Radioactive cesium deposition on rice, wheat, peach tree and soil after nuclear accident in Fukushima. *J Radioanal Nucl Chem* 296:985–989. <https://doi.org/10.1007/s10967-012-2154-7>
  9. Nemoto K, Abe J (2013) Radiocesium absorption by rice in paddy field ecosystems. In: *Agricultural implications of the Fukushima nuclear accident*. Springer Japan, Tokyo, pp 19–27
  10. Suzuki Y, Yasutaka T, Fujimura S et al (2015) Effect of the concentration of radiocesium dissolved in irrigation water on the concentration of radiocesium in brown rice. *Soil Sci Plant Nutr* 61:191–199. <https://doi.org/10.1080/00380768.2014.1003192>
  11. Endo S, Kajimoto T, Shizuma K (2013) Paddy-field contamination with  $^{134}\text{Cs}$  and  $^{137}\text{Cs}$  due to Fukushima Dai-ichi Nuclear Power Plant accident and soil-to-rice transfer coefficients. *J Environ Radioact* 116:59–64. <https://doi.org/10.1016/j.jenvrad.2012.08.018>
  12. Nagao S, Kanamori M, Ochiai S et al (2013) Export of  $^{134}\text{Cs}$  and  $^{137}\text{Cs}$  in the Fukushima river systems at heavy rains by Typhoon Roke in September 2011. *Biogeosci Discuss* 10:2767–2790. <https://doi.org/10.5194/bgd-10-2767-2013>
  13. Kurikami H, Kitamura A, Yokuda ST, Onishi Y (2014) Sediment and  $^{137}\text{Cs}$  behaviors in the Ogaki Dam Reservoir during a heavy rainfall event. *J Environ Radioact* 137:10–17. <https://doi.org/10.1016/j.jenvrad.2014.06.013>
  14. Yoshimura K, Onda Y, Sakaguchi A et al (2015) An extensive study of the concentrations of particulate/dissolved radiocaesium derived from the Fukushima Dai-ichi Nuclear Power Plant accident in various river systems and their relationship with catchment inventory. *J Environ Radioact* 139:370–378. <https://doi.org/10.1016/j.jenvrad.2014.08.021>
  15. Zhu YG, Smolders E (2000) Plant uptake of radiocaesium: a review of mechanisms, regulation and application. *J Exp Bot* 51:1635–1645. <https://doi.org/10.1093/jexbot/51.351.1635>
  16. Tsuji H, Yasutaka T, Kawabe Y et al (2014) Distribution of dissolved and particulate radiocesium concentrations along rivers and the relations between radiocesium concentration and deposition after the nuclear power plant accident in Fukushima. *Water Res* 60:15–27. <https://doi.org/10.1016/j.watres.2014.04.024>
  17. Ashraf MA, Akib S, Maah MJ et al (2014) Cesium-137: radiochemistry, fate, and transport, remediation, and future concerns. *Crit Rev Environ Sci Technol* 44:1740–1793. <https://doi.org/10.1080/10643389.2013.790753>
  18. Mensah AD, Terasaki A, Aung HP et al (2020) Influence of soil characteristics and land use type on existing fractions of radioactive  $^{137}\text{Cs}$  in Fukushima soils. *Environ MDPI* 7:1–13. <https://doi.org/10.3390/environments7020016>
  19. Tanaka K, Iwatani H, Takahashi Y et al (2013) Investigation of spatial distribution of radiocesium in a paddy field as a potential sink. *PLoS ONE* 8:e80794
  20. Yang B, Onda Y, Wakiyama Y et al (2016) Temporal changes of radiocesium in irrigated paddy fields and its accumulation in rice plants in Fukushima. *Environ Pollut* 208:562–570. <https://doi.org/10.1016/j.envpol.2015.10.030>
  21. Sakai M, Gomi T, Nunokawa M et al (2014) Soil removal as a decontamination practice and radiocesium accumulation in tadpoles in rice paddies at Fukushima. *Environ Pollut* 187:112–115. <https://doi.org/10.1016/j.envpol.2014.01.002>
  22. Yang B, Onda Y, Ohmori Y et al (2017) Effect of topsoil removal and selective countermeasures on radiocesium accumulation in rice plants in Fukushima paddy field. *Sci Total Environ* 603–604:49–56. <https://doi.org/10.1016/j.scitotenv.2017.06.026>
  23. Yoshikawa N, Nakashima K, Suzuki Y et al (2020) Influence of irrigation water intake on local increase of radiocesium activity concentration in rice plants near a water inlet. *J Environ Radioact* 225:106441. <https://doi.org/10.1016/j.jenvrad.2020.106441>
  24. Akimoto K (2012) Time- and position dependence in Fukushima prefecture of air dose rate of cs-origin due to the accident at the Fukushima Daiichi Nuclear Power Plant. *Radioisotopes* 61:373–378. <https://doi.org/10.3769/radioisotopes.61.373> **(In Japanese with English abstract)**
  25. Chino M, Nakayama H, Nagai H et al (2011) Preliminary estimation of release amounts of  $^{131}\text{I}$  and  $^{137}\text{Cs}$  accidentally discharged from the Fukushima Daiichi Nuclear Power Plant into the atmosphere. *J Nucl Sci Technol* 48:1129–1134. <https://doi.org/10.1080/18811248.2011.9711799>
  26. Fukushima Prefecture (2019) Fertilization standard in Fukushima prefecture. <https://www.pref.fukushima.lg.jp/sec/36021d/kanky-ou-nogyou-sehikijyun.html> Accessed 27 May 2022 **(In Japanese)**
  27. Kato H, Onda Y, Teramaga M (2012) Depth distribution of  $^{137}\text{Cs}$ ,  $^{134}\text{Cs}$ , and  $^{131}\text{I}$  in soil profile after Fukushima Dai-ichi Nuclear Power Plant accident. *J Environ Radioact* 111:59–64. <https://doi.org/10.1016/j.jenvrad.2011.10.003>
  28. Fujimura S, Yoshioka K, Saito T et al (2013) Effects of applying potassium, zeolite and vermiculite on the radiocesium uptake by rice plants grown in paddy field soils collected from Fukushima prefecture. *Plant Prod Sci* 16:166–170
  29. Kato N, Kihou N, Fujimura S et al (2015) Potassium fertilizer and other materials as countermeasures to reduce radiocesium levels in rice: Results of urgent experiments in 2011 responding to the Fukushima Daiichi Nuclear Power Plant accident. *Soil Sci Plant Nutr* 61:179–190. <https://doi.org/10.1080/00380768.2014.995584>
  30. Kubo K, Fujimura S, Kobayashi H et al (2017) Effect of soil exchangeable potassium content on cesium absorption and partitioning in buckwheat grown in a radioactive cesium-contaminated field. *Plant Prod Sci* 20:396–405. <https://doi.org/10.1080/1343943X.2017.1355737>
  31. Kurokawa K, Nakao A, Tsukada H et al (2019) Exchangeability of  $^{137}\text{Cs}$  and K in soils of agricultural fields after decontamination in the eastern coastal area of Fukushima. *Soil Sci Plant Nutr* 65:401–408. <https://doi.org/10.1080/00380768.2019.1622402>
  32. Rai H, Kawabata M (2020) The dynamics of radio-caesium in soils and mechanism of cesium uptake into higher plants: newly elucidated mechanism of cesium uptake into rice plants. *Front Plant Sci* 11:80–90. <https://doi.org/10.3389/fpls.2020.00528>

**Publisher's Note** Springer Nature remains neutral with regard to jurisdictional claims in published maps and institutional affiliations.

Springer Nature or its licensor holds exclusive rights to this article under a publishing agreement with the author(s) or other rightsholder(s); author self-archiving of the accepted manuscript version of this article is solely governed by the terms of such publishing agreement and applicable law.